SMS overexpression and knockdown: impact on cellular sphingomyelin and diacylglycerol metabolism, and cell apoptosis

Tinbo Ding,* Zhiqiang Li,† Tiruneh Hailemariam,† Sushmita Mukherjee,§ Frederick R. Maxfield,§ Man-Ping Wu,[1,*] and Xian-Cheng Jiang[1,†]

Department of Anatomy and Cell Biology,† State University of New York Downstate Medical Center, Brooklyn, NY 11203; School of Pharmacy,* Fudan University, Shanghai, The People's Republic of China; and Department of Biochemistry,§ Weill Medical College of Cornell University, New York, NY 10065

Abstract Sphingomyelin synthase (SMS), the last enzyme in the sphingomyelin (SM) biosynthetic pathway, uses ceramide and phosphatidylcholine as substrates to produce SM and diacylglycerol (DAG). To evaluate the role of SMS in apoptosis, we generated Chinese hamster ovary cells that stably express human *SMS1* or *SMS2*. We found that *SMS1* or *SMS2* overexpression results in a significant increase in cellular levels of SM (24% or 20%) and DAG (35% or 31%), respectively, compared with controls. Cells overexpressing *SMS1* or *SMS2* were more likely to undergo lysis mediated by lysenin (a protein that causes lysis through its affinity with SM-rich microdomains in the plasma membrane) than were controls, indicating SM enrichment of the plasma membrane. *SMS1* and *SMS2* overexpression also led to higher retention of DiIC16 fluorescence compared with wild-type cells, indicating an increased number of detergent-insoluble microdomains and significantly increased tumor necrosis factor-α-mediated apoptosis. To further evaluate the relationship between SMS activity and cell apoptosis, we used *SMS1* and *SMS2* small interfering RNA (siRNA) to knock down their mRNA in THP-1-derived macrophages. We found that *SMS1* or *SMS2* siRNA significantly reduces intracellular SM (by 20% or 23%), plasma membrane SM (as indicated by the rate of lysenin-mediated cell lysis), and DAG levels (24% or 20%), respectively, while significantly reducing lipopolysaccharide-mediated apoptosis compared with controls. These results indicate that SMS1 and SMS2 are key factors in the control of SM and DAG levels within the cell and thus influence apoptosis.—Ding, T., Z. Li, T. Hailemariam, S. Mukherjee, F. R. Maxfield, M-P. Wu, and X-C. Jiang. **SMS overexpression and knockdown: impact on cellular sphingomyelin and diacylglycerol metabolism, and cell apoptosis. *J. Lipid Res.* 2008.** 49: **376–385.**

Supplementary key words sphingomyelin synthase • siRNA • plasma membrane

Sphingomyelin synthase (SMS) is the last enzyme in the sphingomyelin (SM) biosynthetic pathway. It uses ceramide and phosphatidylcholine (PC) as substrates to produce SM and diacylglycerol (DAG) (1). There are two isoforms of mammalian SMS: SMS1, located on the *cis*-medial aspect of the Golgi apparatus, and SMS2, located on the plasma membrane (2). It is conceivable that manipulation of both SMS1 and SMS2 could influence the metabolism of all four of the structurally important or bioactive lipids.

SM interacts with cholesterol and glycosphingolipid to drive the formation of plasma membrane rafts or detergent-insoluble microdomains (3, 4). Recently, the raft domain has drawn an extensive amount of attention, because it may play an important role as a platform for signal transduction and protein sorting in cellular membranes (5, 6). Yamaoka et al. (7) observed defective cell growth in a mouse lymphoid cell line with no SMS activity and with an SM deficiency and determined that this defect could be corrected through exposure to exogenous SM. Recently, Nagao et al. (8) reported that an SM deficiency in Chinese hamster ovary (CHO) cells enhances ABCA1-mediated cholesterol efflux (the first step in reverse cholesterol transport) and that exposure to exogenous SM can inhibit this process. Tafesse et al. (9) showed that SMS activity in the cell membrane is required for HeLa cell growth. Van der Luit et al. (10) revealed that down-regulation of SMS1 results in an SM-cholesterol deficiency

Manuscript received 5 September 2007 and in revised form 29 October 2007.

Published, JLR Papers in Press, November 2, 2007.
DOI 10.1194/jlr.M700401-JLR200

Abbreviations: CHO, Chinese hamster ovary; DAG, diacylglycerol; FACS, fluorescence-activated cell sorting; KO, knockout; LPS, lipopolysaccharide; PC, phosphatidylcholine; PC-PLC, phosphatidylcholine-phospholipase C; PI-PLC, phosphatidylinositol-phospholipase C; PKC, protein kinase C; PMA, phorbol 12-myristate 13-acetate; SMS, sphingomyelin synthase; SNK, Student-Newman-Keuls; SPT, serine palmitoyl-CoA transferase.

[1] To whom correspondence should be addressed.
e-mail: XJiang@downstate.edu (X-C.J.);
mpwu@shmu.edu.cn (M.W.)

in lipid rafts and attenuates apoptosis induced by alkyllysophospholipid, and that this defect could not be corrected by adding exogenous SM. In a previous study (11), we showed that both SMS1 and SMS2 contribute to de novo SM synthesis and control SM levels in the cell and on cell membranes, including the plasma membrane. All of these findings suggest that an important relationship exists between SMS activity and plasma membrane SM levels and thus between SMS activity and cell function.

The generation of DAG and subsequent protein kinase C (PKC) activation mediates apoptotic activity (12). There are three pathways linking the generation of DAG: (1) catalysis by phosphatidylinositol-phospholipase C (PI-PLC); (2) catalysis by phosphatidylcholine-PLC (PC-PLC); and (3) catalysis by SMS (13). The function of the DAG generated by PI-PLC and PC-PLC activity has been investigated in numerous studies (13). Whether the DAG generated by SMS regulates cellular processes is, in fact, not known. In mammalian cells, SMS activation correlates with the activation and nuclear translocation of NFκB (14); these events are often regulated by DAG-dependent PKC (15). Cerbon and del Carmen Lopez-Sanchez (16) reported that exposure to D609 (an SMS inhibitor) significantly reduces cellular DAG levels, thereby reducing cell proliferation. In a previous study (11), we found that exposure to *SMS1* and *SMS2* small interfering RNA (siRNA) results in lower DAG levels in Huh7 cells, a human hepatoma cell line.

In this study, we investigated the relationship between SMS activity and plasma membrane SM and cellular DAG levels, as well as cell apoptosis. Using gene overexpression and knockdown techniques, we found that *SMS* overexpression significantly increases intracellular SM and DAG levels and increases the rate of apoptosis. We also observed that *SMS1* and *SMS2* knockdown results in a significant reduction in intracellular levels of SM and DAG, as well as a reduction in apoptosis.

MATERIALS AND METHODS

Cell culture

CHO cells were cultured in complete medium (DMEM supplemented with 10% fetal bovine serum). THP-1 cells (American Type Culture Collection), which comprise a human monocytic cell line that differentiates into macrophages in the presence of phorbol 12-myristate 13-acetate (PMA), were maintained in RPMI 1640 medium containing 10% FBS. Using a method described previously (17), we exposed the THP-1 monocytes to 160 nM of PMA (Sigma-Aldrich; St. Louis, MO) for 72 h to induce their differentiation into macrophages.

Preparation of cell lines stably expressing SMS1 or SMS2

Either a pcDNA-SMS1 or a pcDNA-SMS2 (Invitrogen; Carlsbad, CA) plasmid was transferred into the CHO cells with lipofectamine 2000 under standard conditions according to the manufacturer's instructions. G418 was added to the medium 24 h after transfection, to a final concentration of 600 μg/ml, to select cells in which transfection had been successful. Single clones were isolated and subjected to real-time polymerase chain reaction (PCR). An assay of SMS activity was then performed to confirm the overexpression of *SMS1* and *SMS2*.

Quantification of gene expression by real-time PCR

Total RNA was extracted from cells using Trizol (Invitrogen; Carlsbad, CA), and cDNA was synthesized using a kit (Invitrogen). PCR was performed in triplicate using the SYBR® Green PCR Master Mix kit (Applied Biosystems; Foster City, CA); β-actin was used as an internal control. The amplification program consisted of activation at 95°C for 10 min, followed by 40 amplification cycles, each consisting of 95°C for 15 s then 60°C for 1 min. The primers used for the analyses were *SMS1* sense (5′ CAACATTGGCGTAGACAT 3′), *SMS1* antisense (5′ TAGGAGGTACTCGTTCGTG 3′), *SMS2* sense (5′ GATACAAGTCAATAGTGGGACG 3′), *SMS2* antisense (5′ AGAAGTGACGAGGCGAAT 3′), *caspase-3* sense (5′ GGCATTGAGACAGACAGTGG-3′), *caspase-3* antisense (5′ CATGGAATCTGTTTCTTTGC-3′), *β-actin* sense (5′ GGGTCACCCACACTGTGCCCATCTA 3′), and *β-actin* antisense (5′ GCATTTGCGGTGGACGATGGAGG 3′).

Western blot analysis

Equal amounts of cell homogenates (20 μg protein/lane) were separated on 7.5% precast Tris-HCl gels (Bio-Rad; Hercules, CA) under denaturing conditions. Proteins were electroblotted to a nitrocellulose membrane that had been incubated with anti-caspase-3 antibody (Cell Signaling). The loading control was glyceraldehyde-3-phosphate dehydrogenase.

Sphingomyelin synthase activity assay

Cells were homogenized in a buffer containing 50 mM Tris-HCl, 1 mM EDTA, 5% sucrose, and protease inhibitors. The homogenate was centrifuged at 5,000 rpm for 10 min, and the supernatant was used to assay SMS activity. The reaction system contained 50 mM Tris-HCl (pH 7.4), 25 mM KCl, C_6-NBD-ceramide (0.1 μg/μl), and PC (0.01 μg/μl). The mixture was incubated at 37°C for 2 h. Lipids were extracted in chloroform-methanol (2:1), dried under nitrogen gas, and separated using thin layer chromatography (TLC). The plate was scanned with a PhosphorImager (Molecular Dynamics; Sunnyvale, CA), and the intensity of each band was measured using Image-Pro Plus version 4.5 software (Media Cybernetics, Inc.).

Annexin V assay

Wild-type CHO cells (CHO-WT) and CHO cells overexpressing *SMS1* (CHO-SMS1) or *SMS2* (CHO-SMS2) were each subcultured in triplicate to the same density on 12-well plates. When 90% to 100% confluence was achieved, the medium was changed to DMEM (without FBS) with tumor necrosis factor (TNF)-α at a final concentration of 0.4 μg/ml. Cells were incubated for 48 h and then harvested with 0.25% trypsin in phosphate-buffered saline (PBS). The cells were washed twice in PBS and collected by centrifugation at 4°C at 450 *g* for 5 min. They were then stained with fluorescein isothiocyanate-annexin V and propidium iodide according to the manufacturer's instructions. Labeled cells were detected using flow cytometry.

Each group of THP-1-derived macrophages (including those containing control siRNA, *SMS1* siRNA, *SMS2* siRNA, and *SMS1* and *SMS2* siRNA) was analyzed in triplicate. Sixty hours after siRNA transfection, the cells were quickly washed twice with PBS, and then complete medium RPMI-1640 containing 100 ng/ml lipopolysaccharide (LPS) was added to each group of cells. After 1.5 h of LPS exposure, the cells were harvested with 0.25% trypsin in PBS. The cell staining and flow cytometry detection methods used with these cells were the same as those used with the CHO cells.

Cold triton extraction and DilC16 fluorescence intensity measurement

Cells were prepared for microscopy with 2 days in culture consisting of Ham's F12 medium supplemented with 5% FBS, at 37°C in a 5% CO_2 humidified incubator, in 35 mm plastic tissue culture dishes, the bottoms of which had been replaced with poly-D-lysine-coated coverslips, as described by Salzman and Maxfield (18). On the day of the experiment, the medium was changed to prewarmed Medium 1 (150 mM NaCl, 20 mM HEPES, 1 mM $CaCl_2$, 5 mM KCl, 1 mM $MgCl_2$, and 2 g/l glucose), and the cells were equilibrated at 37°C in a bench-top warmer for a few minutes. The cells were then labeled with DiIC16 and loaded onto fatty-acid-free BSA for 30 s at 37°C using established protocols (19). Following the labeling procedure, the cells were washed three times with chilled Medium 1 and incubated in an ice-water chamber maintained at approximately 0°C for at least 10 min. The cells were then treated with 1% Triton X-100 (in Medium 1) for 5 min at 0°C. After the extraction, the cells were washed three times with chilled Medium 1 and held for 15 min at 0°C. The cells were then warmed to room temperature just prior to imaging. Digital image acquisition was carried out using a Leica DMIRB microscope (Leica Mikroscopie und Systeme; GmbH, Wetzlar, Germany) equipped with a Princeton Instruments (Princeton, NJ) cooled, charge-coupled device camera driven by MetaMorph Imaging System software (Universal Imaging Corporation; Downington, PA). Standard rhodamine filters were used for imaging with DiIC16. All imaging was done with a low-power (10×, NA 0.3) objective in order to visualize a large number of cells in each field. The background in each image was corrected by subtracting the intensity of unlabeled cells that had been cultured and imaged under conditions identical to those used in the experimental procedure. After background correction, the images were thresholded to reject any unsubtracted noncell-associated fluorescence, and the integrated intensity and size of the thresholded area were recorded for each image. The results are expressed as the mean cell-associated fluorescence intensity per field. Data for each condition represent an average of 500 to 2,500 cells. All analyses were done using MetaMorph image analysis software (Universal Imaging Corporation).

Cellular lipid content

The cell monolayer was washed twice with PBS, and cellular lipids were extracted using *n*-hexane-2-propanol (3:2). Aliquots of the extracted lipids were subjected to analysis. The SM and PC content was measured using a method described previously in our laboratory (20). Briefly, the extracted lipids were incubated with bacterial SMase (or PC-phosphalipase D), alkaline phosphatase, choline oxidase, peroxidase, *N*-ethyl-*N*-(2-hydroxy-3-sulfopropyl)-3,5-dimethoxyaniline, and 4-aminoantipyrine for 45 min. The absorbance of generated blue dye was measured by spectrophotometry at 595 nm. Ceramide and DAG levels were measured using the DAG kinase assay, in which the amount of ^{32}P incorporated during phosphorylation of ceramide and DAG to ceramide-1-phosphate and phosphatidic acid by DAG kinase was measured (Sigma-Aldrich). Briefly, γ-^{32}P-ATP (10 mM, 10 μCi) was incubated with the enzyme and lipid samples in an imidazole buffer (pH 6.6), as described by Preiss et al. (21). Ceramide-1-phosphate and phosphatidic acid were resolved by TLC using $CHCl_3$-CH_3OH-CH_3COOH (65:15:5, v/v/v) as a solvent. Ceramide-1-phosphate and phospatidic acid were identified by autoradiography at Rf 0.25 and Rf 0.45, respectively, and quantified by scintillation counting. The ceramide and DAG levels were quantified by comparison with a concomitantly run standard curve representing known amounts of ceramide and DAG and normalized to [^{3}H]triglyceride introduced as an external standard during lipid extraction.

Exogenous addition of SM

SM was dissolved in 2:1 ethanol-Me_2SO to make a 5 mM stock. An aliquot of this stock solution was added to the culture medium to a final concentration of 40 μM as described previously (22), and cells were incubated for 12 h.

Toll-like receptor 4 analyses by fluorescence-activated cell sorting

Cell surface receptors were detected as described previously (23). Briefly, macrophages were stimulated by LPS (100 ng/ml) for 2 min and then stained with 1 μg/ml Toll-like receptor 4 (TLR4)/MD-2 complex antibody (CSA-805FIJ; Stressgen) for 1 h on ice, then washed with ice-cold PBS three times before analysis on a FACScan with CellQuest software (Benton Dickinson).

Statistical analysis

Each experiment was conducted at least five times. Data are typically expressed as mean ± SD. Data between two groups were analyzed by Student's *t*-test and among multiple groups by ANOVA followed by the Student-Newman-Keuls (SNK) test. A *P* value of less than 0.05 was considered significant.

RESULTS

SMS1 and SMS2 overexpression increases CHO cell SMS activity and plasma membrane SM levels

To investigate the role of SMS1 and SMS2, we established two stable CHO cell lines that express human *SMS1* (SMS1-CHO) and *SMS2* (SMS2-CHO). Real-time PCR was performed on RNA prepared from both cells and revealed a 2.5-fold increase in *SMS1* mRNA levels and a 2.3-fold increase in *SMS2* mRNA levels, respectively, compared with control CHO cells. The cellular SMS activity assay was also measured in SMS1-CHO, SMS2-CHO, and control CHO cells. *SMS1* overexpression resulted in a 2.2-fold increase in cellular SMS activity, and *SMS2* overexpression resulted in a 1.85-fold increase compared with controls (**Fig. 1A, B**).

We used enzymatic assays to determine whether overexpression of *SMS1* and *SMS2* had any effect on cellular lipid levels, including SM, PC, ceramide, and DAG levels. As indicated in **Table 1**, cells in which *SMS1* or *SMS2* was overexpressed contained significantly higher SM levels (24% and 20%, respectively; $P < 0.05$). Interestingly, ceramide levels (44% and 42%, respectively) and the ceramide:sphingomyelin ratio (18% and 18%, respectively) increased significantly compared with controls ($P < 0.01$ and $P < 0.05$, respectively). As expected, cellular DAG levels also increased significantly (35% and 31%, respectively; $P < 0.01$) in both SMS-overexpressing cells. Differences in cellular PC levels among the cell groups were not significant.

Because cellular SM levels represent SM levels in all cellular membranes, including plasma membrane, endoplasmic reticulum, and Golgi complex, we still do not know whether *SMS1* or *SMS2* overexpression has an effect

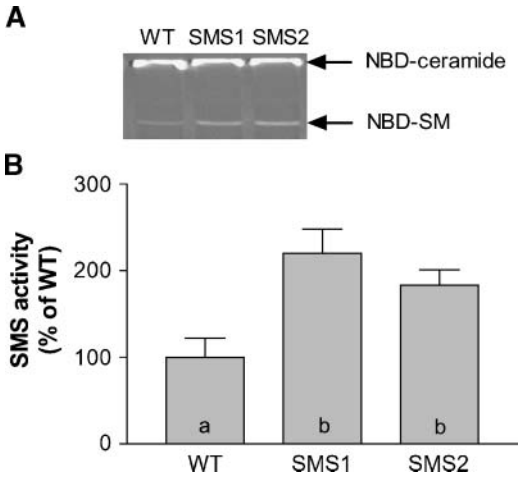

Fig. 1. Sphingomyelin synthase activity assay. The SMS1-CHO, SMS2-CHO, and WT-CHO cells were homogenized. The reaction system contained cell homogenate (200 μg protein), C6-NBD-ceramide, and PC. The mixture was incubated at 37°C for 2 h. Lipids were extracted in chloroform-methanol (2:1), dried under N_2 gas, and then separated using thin layer chromatography (TLC). The fluorescent intensity of each spot was determined as described in the Materials and Methods section of this article. A: Nitro-2-1,3-BenzoxaDiazol-4-yl-SM fluorogram, which is representative of independent experiments. B: Quantitative display of SMS activity (mean ± SD; N = 5). $P < 0.001$ by ANOVA; $P < 0.01$ by Student-Newman-Keuls (SNK) procedure. Columns labeled with different lower-case letters are statistically different by the SNK test.

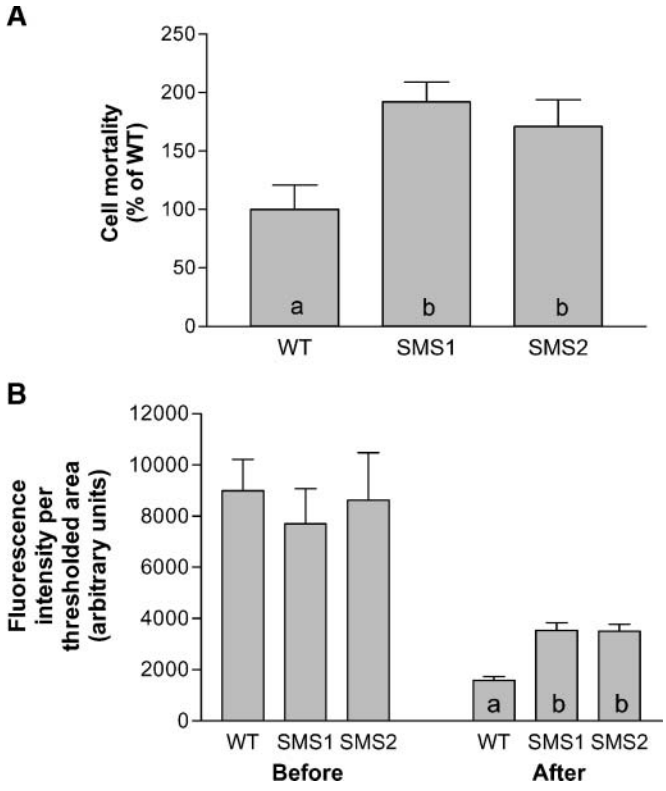

Fig. 2. *SMS1* and *SMS2* overexpression altered plasma membrane SM levels. A: *SMS1* and *SMS2* overexpression increased lysenin-mediated cell mortality. Lysenin (200 ng/ml) was added to the culture medium containing SMS1-CHO, SMS2-CHO, and WT-CHO cells. Cell mortality was monitored with WST-1 Cell Proliferation Reagent (Roche; Basel, Switzerland). B: *SMS1* and *SMS2* overexpression increased the proportion of detergent-resistant raft-like domains at the plasma membrane. Details of this procedure are described in the Materials and Methods section of this article. Before, before cold Triton X-100 extraction; After, after cold Triton X-100 extraction. In both A and B, $P < 0.001$ by ANOVA and $P < 0.01$ by SNK test. Columns labeled with different lower-case letters are statistically different by the SNK test.

on SM levels specifically in the plasma membrane, where all signal transduction is initiated. Lysenin is a recently discovered SM-specific cytotoxin that recognizes SM only when it forms aggregates or microdomains (24). To investigate the effect of *SMS1* or *SMS2* overexpression on the formation of these microdomains, we tested SMS1-CHO and SMS2-CHO cells for their sensitivity to lysenin-mediated cytolysis. As indicated in **Fig. 2A**, both SMS1-CHO and SMS2-CHO cells showed significantly more sensitivity to lysenin-mediated cytolysis than did WT-CHO cells.

Cholesterol- and SM-enriched membrane regions are known as liquid-ordered domains, or "rafts." (3). Such regions are relatively insoluble in cold Triton X-100 (25). We considered the possibility that *SMS1* or *SMS2* overexpression might change the overall organization of the plasma membrane. The presence of liquid-ordered domains was assessed by wide-field fluorescence microscopy, through which we observed the incorporation of the fluorescent phospholipid analog DiIC16 into the plasma membranes of intact cells. We found that DiIC16 labeled the plasma membranes of all tested cell lines almost equally well; however, upon cold triton extraction, roughly 50% more cells associated with DiIC16 were retained by the SMS1-CHO and SMS2-CHO cells com-

TABLE 1. Lipid concentrations in CHO cells overexpressing *SMS1* and *SMS2*

Type of Cell	SM	PC	Cer	DAG	Cer:SM
			nmol/mg protein		
Control	25 ± 3	294 ± 23	0.96 ± 0.09	2.45 ± 0.51	0.038 ± 0.002
Overexpressing *SMS1*	31 ± 3[a]	283 ± 37	1.38 ± 0.08[a]	3.31 ± 0.66[a]	0.045 ± 0.003[a]
Overexpressing *SMS2*	30 ± 2[a]	280 ± 46	1.36 ± 0.11[a]	3.21 ± 0.39[a]	0.045 ± 0.004[a]

Cer, ceramide; CHO, Chinese hamster ovary; DAG, diacylglycerol; PC, phosphatidylcholine; SM, sphingomyelin; SMS, sphingomyelin synthase. Data are given as mean ± SD and are the average of five experiments.

[a] Statistically significant compared with control in the same column; $P < 0.01$ by ANOVA and $P < 0.05$ by Student-Newman-Keuls test.

pared with the WT-CHO cells (Fig. 2B). These results indicate that *SMS* overexpression increases the raft-like domains in the plasma membrane.

SMS1 and SMS2 overexpression increases TNF-α-induced apoptosis in CHO cells

We next sought to determine whether overexpression of *SMS1* and *SMS2* in CHO cells contributes to apoptosis induced by TNF-α. As stated above, there is evidence that cells that are deficient in SMS1 and therefore depleted of SM in lipid rafts are resistant to alkyl-lysophospholipid-induced apoptosis (10). We therefore reasoned that overexpression of *SMS1* or *SMS2* might increase TNF-α-induced apoptosis by increasing SM levels in the plasma membrane. Indeed, we found that after TNF-α stimulation, the proportion of apoptotic SMS1-CHO and SMS2-CHO cells increased significantly, by 56% and 37% ($P < 0.01$), respectively, compared with WT-CHO cells (**Fig. 3A, B**). To confirm this phenomenon, we measured caspase-3 (well known for its involvement in apoptosis) (26) mRNA levels and its active protein mass and found that *SMS1* and *SMS2* overexpression resulted in a significant increase in the enzyme mRNA levels (2.4-fold and 2.0-fold, respectively; $P < 0.01$) (Fig. 3C) and in the concentration of cleaved caspase-3 (the active form of the enzyme), 2.2- and 1.8-fold, respectively ($P < 0.01$) compared with WT-CHO cells (Fig. 3D, E).

SMS1 and SMS2 siRNA decreases SMS activity and plasma membrane SM levels in THP-1-derived macrophages

We used siRNA to investigate further the relationship between SMS and SM levels and the potential differences between SMS1 and SMS2 genes. The reasons to choose THP-1-derived macrophages are: *1*) they are human macrophages; *2*) macrophage apoptosis is related to the development of atherosclerosis; and *3*) because hamster

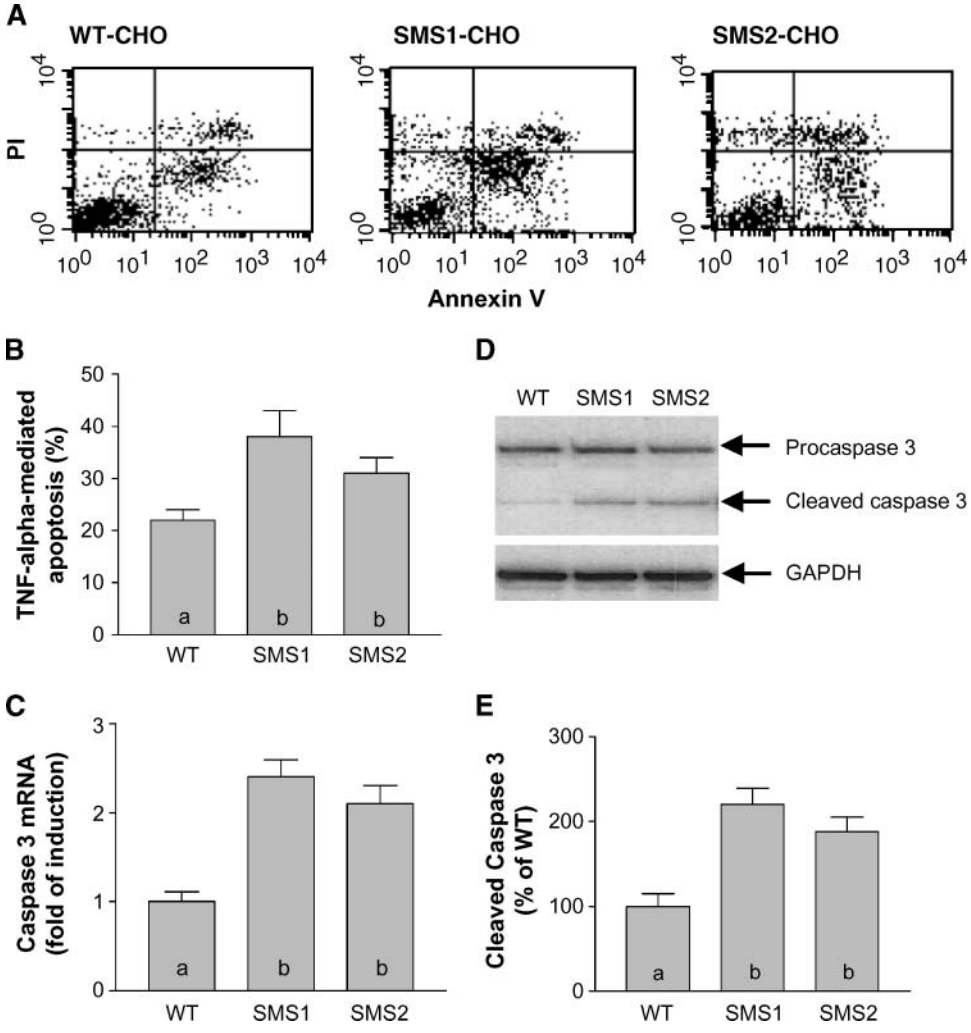

Fig. 3. *SMS1* and *SMS2* overexpression increased CHO cell apoptosis. A: A representation of independent annexin V assays. B: Quantitative display of annexin V assays. C: Quantitative display of *caspase-3* mRNA real-time PCR analysis. D: A representation of caspase-3 Western blot analysis. E: Quantitative display of caspase-3 protein mass. Data are displayed as the mean ± SD (N = 5). In B, C, and E, $P < 0.001$ by ANOVA and $P < 0.01$ by SNK test. Columns labeled with different lower-case letters are statistically different by the SNK test.

SMS1 and SMS2 cDNA sequences are not known, the siRNA approach to knockdown SMS1 and SMS2 in CHO cells is not yet plausible. We treated THP-1 cells with PMA for 72 h to induce macrophage formation (17) and then treated the macrophages with *SMS1*, *SMS2*, or scrambled siRNA. We found that exposure to *SMS1* or *SMS2* siRNA caused a significant decrease in SMS activity (23% and 29%, respectively; $P < 0.01$) (**Fig. 4A**) and a significant decrease in lysenin-mediated cell mortality (28% and 35%, respectively; $P < 0.01$) (Fig. 4B) compared with controls, indicating that SMS1 or SMS2 gene knockdown not only reduces cellular SMS activity but also reduces SM levels in the plasma membrane. The combination of both siRNAs had an additive effect on both SMS activity and plasma membrane SM levels (Fig. 4A, B).

We also measured cellular lipid levels by enzymatic analysis. As indicated in **Table 2**, the total SM was significantly lower in cells that had been transfected with *SMS1* siRNA, *SMS2* siRNA, or a combination of these siRNAs compared with control siRNA-transfected cells [20% ($P < 0.05$), 23% ($P < 0.01$), and 25% ($P < 0.01$), respectively], whereas little or no change was seen in ceramide levels. There was a significant decrease in cellular DAG levels [24% ($P < 0.01$), 20% ($P < 0.05$), and 25% ($P < 0.01$), respectively], whereas there was no significant change in the differences in cellular PC levels.

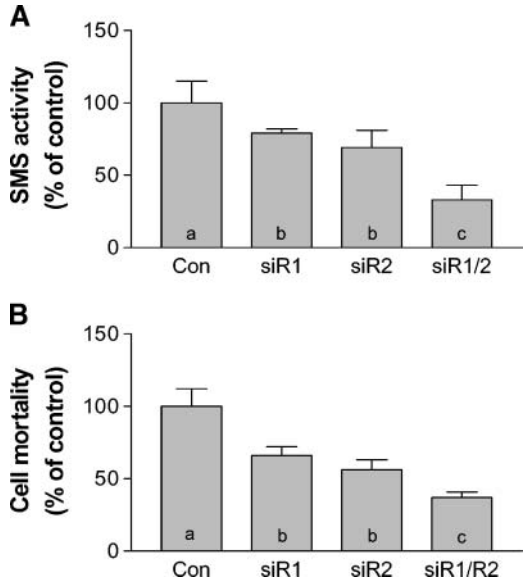

Fig. 4. SMS1 and SMS2 knockdown decreased SMS activity and reduced plasma membrane SM levels. A: Quantitative display of SMS activity. The SMS1 siRNA-, SMS2 siRNA-, and control siRNA-treated macrophages were homogenized. The reaction system contained cell homogenate (200 μg protein), C6-NBD-ceramide, and PC. The mixture was incubated at 37°C for 2 h. Lipids were extracted in chloroform-methanol (2:1), dried under N_2 gas, then separated by TLC. The fluorescent intensity of each spot was determined as described in the Materials and Methods section of this article. B: Quantitative display of lysenin-mediated cell lysis. Lysenin (200 ng/ml) was added to the culture medium containing SMS1 siRNA-, SMS2 siRNA-, and control siRNA-treated macrophages. Data are displayed as the mean ± SD (N = 5). In A and B, $P < 0.001$ by ANOVA and $P < 0.01$ by SNK test. Con, control siRNA; siR1, SMS1 siRNA; siR2, SMS2 siRNA; siR1/R2, SMS1/2 siRNAs. Columns labeled with different lower-case letters are statistically different by the SNK test.

SMS1 and *SMS2* gene knockdown decreases LPS-induced apoptosis in THP-1-derived macrophages

We next sought to determine whether *SMS1* and *SMS2* knockdown in THP-1-derived macrophages contributes to apoptosis induced by LPS. We found that after LPS stimulation, the number of apoptotic macrophages decreased by 21% ($P < 0.05$) and 41% ($P < 0.01$), respectively, compared with controls (**Fig. 5A, B**). An additive effect was observed after the macrophages were exposed to both *SMS1* and *SMS2* siRNA (Fig. 5B).

To determine whether the reduced LPS-induced apoptosis was due to the lack of SMS activity or to the lack of SM in plasma membrane lipid rafts, we loaded *SMS1/2* knockdown macrophages with exogenous SM. As indicated in Fig. 5C, *SMS1/SMS2* siRNA treatment significantly attenuates LPS-induced apopotosis, compared with controls, and this defect cannot be corrected by adding exogenous SM, suggesting that SM synthesis, rather than mere SM accumulation in lipid rafts at the plasma membrane, could influence LPS-induced apoptosis.

We next measured *caspase-3* mRNA levels and its active protein mass to confirm this and found that exposure to both *SMS1* and *SMS2* siRNAs significantly reduced *caspase-3* mRNA levels (37% and 44%, respectively) (Fig. 5D) and active caspase-3 levels (45% and 50%, respectively; each $P < 0.01$) compared with scrambled siRNA (Fig. 5E, F). We also observed an additive effect after these cells were exposed to both *SMS1* and *SMS2* siRNA (Fig. 5F).

To determine whether the depletion of plasma membrane SM levels had an impact on the cell surface expression of the LPS receptor TLR4, we conducted fluorescence-activated cell sorting (FACS) analysis with LPS-stimulated *SMS1/SMS2* knockdown and control macrophages. As shown in **Fig. 6**, after 2 min of LPS stimulation, control macrophages contained more TLR4 on the cell surface than did *SMS1/SMS2* knockdown macrophages.

To further explore the mechanism by which SMS2 affected NFκB, we investigated LPS-induced cell surface recruitment of TLR4 and its coreceptor MD2, a consequence of signaling upstream of NFκB activation (27), in SMS2 knockout (KO) macrophages. As shown in Fig. 6 FACS analysis showed that after 2 min of LPS stimulation, SMS2 KO macrophages contained fewer TLR4/MD2 complexes on the cell surface than did control macrophages. This result indicates that SMS2 is critical for LPS-induced cell surface TLR4 and MD2 recruitment and complex formation.

DISCUSSION

In this study, we demonstrated that *1*) overexpression of both *SMS1* and *SMS2* significantly increases cellular SM and DAG levels and induces TNF-α-mediated CHO cell apoptosis; and *2*) *SMS1* and *SMS2* knockdown sig-

TABLE 2. Lipid concentrations in *SMS1* and *SMS2* knockdown macrophages

Type of Cell	SM	PC	Cer	DAG	Cer:SM
			nmol/mg protein		
Control	44 ± 5	320 ± 33	0.77 ± 0.06	2.26 ± 0.12	0.018 ± 0.003
SMS1 siRNA	35 ± 4[a]	339 ± 19	0.73 ± 0.09	1.71 ± 0.23[a]	0.021 ± 0.004
SMS2 siRNA	34 ± 2[a]	347 ± 36	0.72 ± 0.07	1.81 ± 0.17[a]	0.021 ± 0.003
SMS1/2 siRNA	33 ± 3[a]	327 ± 27	0.73 ± 0.03	1.69 ± 0.11[a]	0.022 ± 0.005

siRNA, small interfering RNA. Data are given as mean ± SD and are the average of five experiments.
[a] Statistically significant compared with control in the same column; $P < 0.01$ by ANOVA and $P < 0.05$ by Student-Newman-Keuls test.

nificantly reduces cellular SM and DAG levels and reduces the rate of LPS-mediated macrophage apoptosis.

SM is a ubiquitous structural component of mammalian cell membranes and lipoproteins whose cellular and plasma levels are regulated by both anabolic and catabolic pathways. The biosynthesis of SM is induced by serine palmitoyl-CoA transferase (SPT, the first enzyme in the SM biosynthetic pathway), 3-ketosphinganine reductase, ceramide synthase, dihydroceramide desaturase, and SMS (the last enzyme in the SM biosynthetic pathway) activity (1). Many reports indicate that SPT is the key enzyme in the biosynthesis of all sphingolipids (1, 28, 29). However,

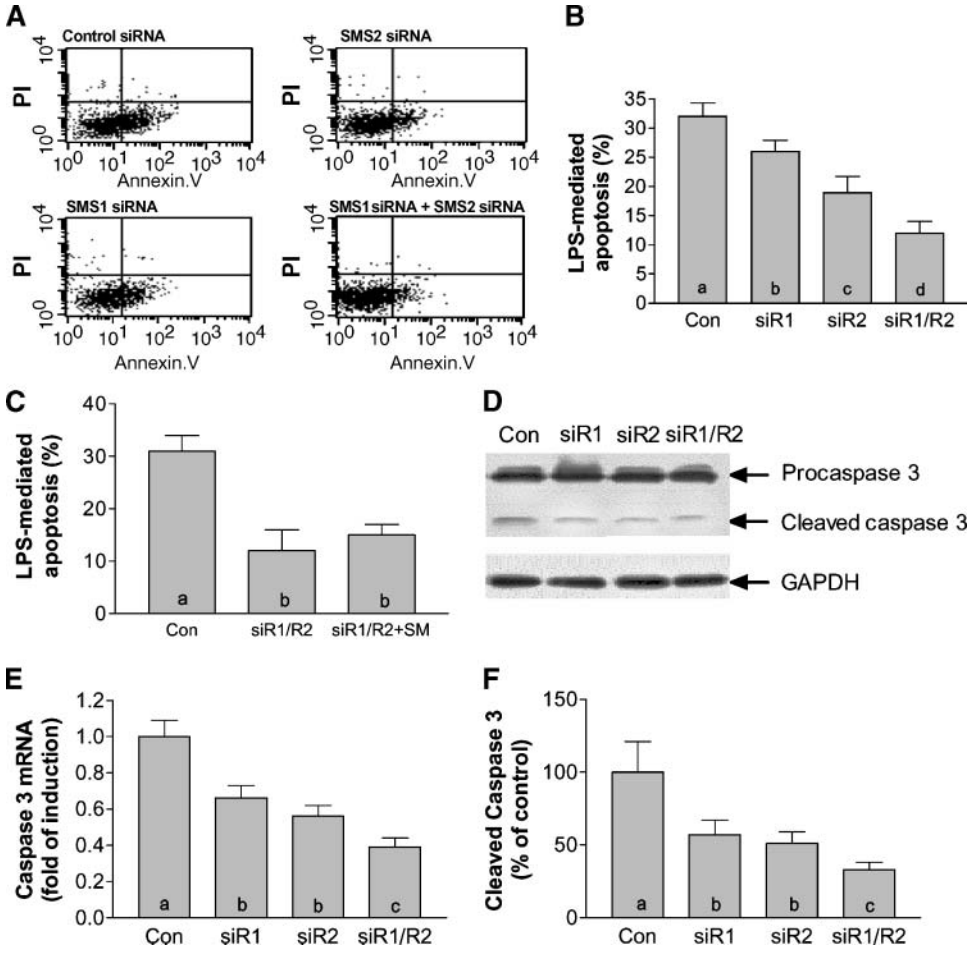

Fig. 5. *SMS1* and SMS2 knockdown decreased macrophage cell apoptosis. Sixty hours after siRNA transfection, the cells were quickly washed twice with PBS, and then complete medium RPMI-1640 containing 100 ng/ml lipopolysaccharide (LPS) was added to each group of cells. A: A representation of independent annexin V assays. B: Quantitative display of annexin V assays. C: Quantitative display of annexin V (control siRNA and SMS1/2 siRNAs.; D: A representation of caspase-3 Western blot analysis. E: Quantitative display of activated caspase-3 levels. F: Quantitative display of caspase-3 protein mass. Data are displayed as mean ± SD (N = 5). In B, C, and E, $P < 0.001$ by ANOVA and $P < 0.01$ by SNK test. Con, control siRNA; siR1, SMS1 siRNA; siR2, SMS2 siRNA; siR1/R2, SMS1/2 siRNAs. Columns labeled with different lower-case letters are statistically different by the SNK test.

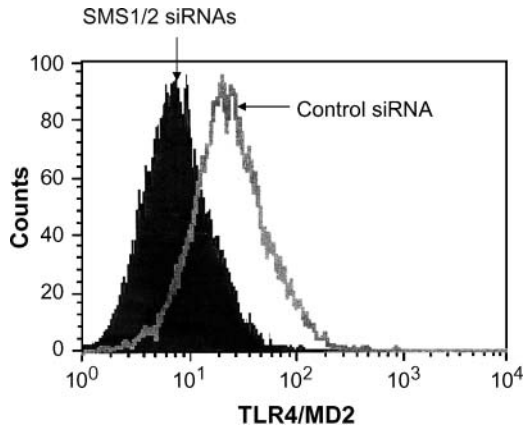

Fig. 6. Reduction of Toll-like receptor 4 (TLR4) on SMS1/SMS2 knockdown macrophages after LPS stimulation. Cell surface receptors were detected as described previously (23). Briefly, control siRNA- or SMS1/2 siRNA-treated macrophages were stimulated by LPS (100 ng/ml) for 2 min and then stained with 1 μg/ml TLR4/MD-2 complex antibody (CSA-805FIJ, Stressgen) for 1 h on ice, then washed with ice-cold PBS three times before analysis on a FACScan with CellQuest software. Data are representative of three independent assays.

there is some evidence that SMS is the key enzyme for SM biosynthesis. This is supported by the observation that cells exposed to D609 (an SMS inhibitor) have significantly reduced SMS activity, which, in turn, is associated with a significant reduction in intracellular levels of SM (30). In a previous study, we found that SMS inhibition, through exposure to either D609 or siRNA, results in a significant reduction in intracellular SM levels (11). A recent study also reported that SMS deficiency leads to SM depletion in S49 mouse lymphoma cells (10).

SMS makes an important contribution to the cell membrane structure, because SM is an important component of membrane lipid rafts (1). Yamaoka et al. (7) isolated mouse lymphoid cells, demonstrating a reduced SM concentration at the plasma membrane owing to the absence of SMS activity and resistance to lysenin-induced cell death. We previously found that approximately 65% of cell membrane-associated SM is located in lipid rafts (11) and that exposure to D609 or siRNA not only reduces cellular SMS activity, but also reduces SM levels in plasma membranes. In this study, we confirmed this observation in THP-1-derived macrophages (Fig. 4A, B). We also found that overexpression of both *SMS1* and *SMS2* increases SM levels in the plasma membrane (Fig. 2A) and in detergent-insoluble regions (lipid rafts) (Fig. 2B). It is believed that plasma membrane rafts represent signaling microdomains. Indeed, it has been reported that downregulation of SMS1 reduces the amount of SM in lipid rafts and reduces the rate of cell apoptosis induced by alkyl-lysophospholipid (10). It has also been reported that D609 exposure inhibits TNF-α- (27, 14) or phorbol ester-mediated (14) NFκB activity. A critical question remains to be answered: are both SMS1 and SMS2 responsible for the production of plasma membrane-associated SM? We found that at least in CHO cells and THP-1-derived macrophages (this study), HEK 293 cells and Huh7 cells [our previous study, (11)], both SMS1 and SMS2 are responsible for SM levels in the plasma membrane.

In two recent papers, investigators reported controversial results regarding the relationship between SMS activity and cell apoptosis. Van der Luit et al. (10) reported that SMS1 gene knockdown alters the plasma membrane raft structure and reduces the internalization of alkyl-lysophospholipid, thereby reducing cell apoptosis rates. Separovic et al. (31) reported that *SMS1* overexpression suppresses cell apoptosis mediated by photo damage; however, they did not show the effect of *SMS1* overexpression on membrane lipid rafts. On the basis of the results of our study, we believe that overexpression of *SMS1* and *SMS2* increases SM levels in the lipid rafts on plasma membranes and promotes a more external appearance for TNF-α receptor 1 (a well-known receptor in lipid rafts) (32) following TNF-α stimulation, thereby promoting CHO cell apoptosis. We also believe that *SMS1* and *SMS2* knockdown by siRNA reduces SM levels in lipid rafts on the plasma membrane and reduces the number of TLR4s (which are also well known for their presence in lipid rafts) (33) that are present on the plasma membrane after LPS stimulation, thereby reducing macrophage apoptosis. Indeed, after LPS stimulation, *SMS1/SMS2* knockdown macrophages contained significantly less TLR4 on the cell surface than did control macrophages (Fig. 6).

Manipulation of SMS activity alters cellular DAG levels and thus may also contribute to apoptosis. Cerbon and del Carmen Lopez-Sanchez (16) demonstrated that pharmacological inhibition of SMS reduces cellular DAG levels and PKC activity. In this study, we found that overexpression of *SMS1* or *SMS2* significantly increases DAG levels in CHO cells (Table 1), whereas *SMS1* or *SMS2* gene knockdown significantly reduces DAG levels in THP-1-derived macrophages (Table 2). DAG can regulate both conventional and novel PKCs (13), a family of serine/threonine kinases that regulate a diverse set of cellular processes, including pro-apoptotic and pro-survival processes. The PKC isozyme has a distinct role in these processes, functioning in a cell type-dependent manner (12). PKCδ is generally considered to be a growth-inhibitory or pro-apoptotic PKC (12, 34), whereas PKCε is considered to be a pro-survival factor (12, 35). It is possible that in both CHO cells and THP-1-derived macrophages, regulation of SMS1 or SMS2 activity by either the overexpression of their genes or gene knockdown could modulate DAG-mediated PKC activity, thereby influencing cell apoptosis. This phenomenon deserves further investigation.

Manipulation of SMS activity also alters cellular ceramide levels, and this may contribute to apoptosis. SMS catalyzes the production of SM and DAG from ceramide and PC, but can also catalyze the reverse reaction (2). Overexpression of both *SMS1* and *SMS2* is accompanied by increased levels of ceramide, as well as SM (Table 1). Separovic et al. (32) observed the same phenomenon when they overexpressed *SMS1* in Jurkat cells. This may be due to the complexity of this enzyme, which can catalyze bidirectional reactions (2). Moreover, we found that

the ceramide:SM ratio increases in cells that overexpress SMS, compared with controls (Table 1). This may represent another mechanism for the increased apoptotic potential of these cells, given that ceramide is a bioactive lipid that is well known for promoting cell apoptosis (36, 37). However, ceramide levels did not change in THP-derived macrophages after they were exposed to SMS siRNA. This indicates that the ceramide level might not be important in SMS knockdown-induced macrophage apoptosis. We also measured sphingomyelinase activity, but found no difference between SMS-overexpressed cells and their controls (data not shown), indicating that sphingomyelinase activity does not make a contribution to the increase of ceramide levels.

Apoptosis is an intrinsic cell suicide mechanism in which a carefully orchestrated pattern of cytoplasmic and nuclear changes results in self-destruction and clearance of individual cells from tissues without provoking an inflammatory response (38). It is believed that disordered apoptosis may occur in atherogenesis, leading to the death of lipid-rich foam cells and promoting lipid core formation (39). However, in reality, the relationship of macrophage apoptosis to atherosclerosis is complex (40). Recent reports have indicated that the net effect of early lesional macrophage apoptosis is modulation of lesion cellularity and decreased lesion progression (40– 42). However, the later development of atherosclerotic lesions leads to the generation of the necrotic core, which promotes plaque instability and acute lesional thrombosis (40). So the late lesional macrophage apoptosis is proatherogenic (40, 43, 44). Whether SMS-induced apoptosis is proatherogenic or antiatherogenic deserves further elucidation.

We conclude that overexpression of SMS leads to a significant increase in SM and DAG levels within CHO cells and promotes TNF-α-mediated apoptosis, whereas an SMS deficiency leads to a significant reduction in SM and DAG levels within the THP-1-derived macrophages and limits LPS-induced apoptosis. These results suggest that both SMS1 and SMS2 regulate intracellular SM and DAG levels and, hence, could contribute to changes in the lipid rafts on the plasma membrane or affect PKC activity in certain disease states (12, 45).

This work was partially supported by National Institutes of Health Grants HL-64735 and HL-69817 (X-C.J), by a Grant-in-aid from the American Heart Association (X-C.J), and by the Young Investigator Start-up Fund of the School of Pharmacy, Fudan University (T.D.).

REFERENCES

1. Merrill, A. H., and D. D. Jones. 1990. An update of the enzymology and regulation of sphingomyelin metabolism. *Biochim. Biophys. ACTA.* **1044:** 1–12.
2. Huitema, K., J. van den Dikkenberg, J. F. Brouwers, and J. C. Holthuis. 2004. Identification of a family of animal sphingomyelin synthases. *EMBO J.* **23:** 33–44.
3. Simons, K., and E. Ikonen. 1997. Functional rafts in cell membranes. *Nature.* **387:** 569–572.
4. Simons, K., and G. van Meer. 1988. Lipid sorting in epithelial cells. *Biochemistry.* **27:** 6197–6202.
5. Brown, D. A., and J. K. Rose. 1992. Sorting of GPI-anchored proteins to glycolipid-enriched membrane subdomains during transport to the apical cell surface. *Cell.* **68:** 533–544.
6. Parton, R. G., and K. Simons. 1995. Digging into caveolae. *Science.* **269:** 1398–1399.
7. Yamaoka, S., M. Miyaji, T. Kitano, H. Umehara, and T. Okazaki. 2004. Expression cloning of a human cDNA restoring sphingomyelin synthesis and cell growth in sphingomyelin synthase-defective lymphoid cells. *J. Biol. Chem.* **279:** 18688–18693.
8. Nagao, K., K. Takahashi, K. Hanada, N. Kioka, M. Matsuo, and K. Ueda. 2007. Enhanced apoA-I-dependent cholesterol efflux by ABCA1 from sphingomyelin-deficient Chinese hamster ovary cells. *J. Biol. Chem.* **282:** 14868–14874.
9. Tafesse, F. G., K. Huitema, M. Hermansson, S. van der Poel, J. van den Dikkenberg, A. Uphoff, P. Somerharju, and J. C. Holthuis. 2007. Both sphingomyelin synthases SMS1 and SMS2 are required for sphingomyelin homeostasis and growth in human HeLa cells. *J. Biol. Chem.* **282:** 17537–17547.
10. van der Luit, A. H., M. Budde, S. Zerp, W. Caan, J. B. Klarenbeek, M. Verheij, and W. J. van Blitterswijk. 2007. Resistance to alkyllysophospholipid-induced apoptosis due to downregulated sphingomyelin synthase 1 expression with consequent sphingomyelin- and cholesterol-deficiency in lipid rafts. *Biochem. J.* **401:** 541–549.
11. Li, Z., T. K. Hailemariam, H. Zhou, Y. Li, D. C. Duckworth, D. A. Peake, Y. Zhang, M. S. Kuo, G. Cao, and X. C. Jiang. 2007. Inhibition of sphingomyelin synthase (SMS) affects intracellular sphingomyelin accumulation and plasma membrane lipid organization. *Biochim. Biophys. Acta.* **1771:** 1186–1194.
12. Griner, E. M., and M. G. Kazanietz. 2007. Protein kinase C and other diacylglycerol effectors in cancer. *Nat. Rev. Cancer.* **7:** 281–294.
13. Wakelam, M. J. 1998. Diacylglycerol—when is it an intracellular messenger? *Biochim. Biophys. Acta.* **1436:** 117–126.
14. Luberto, C., D. S. Yoo, H. S. Suidan, G. M. Bartoli, and Y. A. Hannun. 2000. Differential effects of sphingomyelin hydrolysis and resynthesis on the activation of NF-kappa B in normal and SV40-transformed human fibroblasts. *J. Biol. Chem.* **275:** 14760–14766.
15. Signorelli, P., C. Luberto, and Y. A. Hannun. 2001. Ceramide inhibition of NF-kappaB activation involves reverse translocation of classical protein kinase C (PKC) isoenzymes: requirement for kinase activity and carboxyl-terminal phosphorylation of PKC for the ceramide response. *FASEB J.* **15:** 2401–2414.
16. Cerbon, J., and R. del Carmen Lopez-Sanchez. 2003. Diacylglycerol generated during sphingomyelin synthesis is involved in protein kinase C activation and cell proliferation in Madin-Darby canine kidney cells. *Biochem. J.* **373:** 917–924.
17. Lada, A. T., L. L. Rudel, and R. W. St Clair. 2003. Effects of LDL enriched with different dietary fatty acids on cholesteryl ester accumulation and turnover in THP-1 macrophages. *J. Lipid Res.* **44:** 770–779.
18. Salzman, N. H., and F. R. Maxfield. 1989. Fusion accessibility of endocytic compartments along the recycling and lysosomal endocytic pathways in intact cells. *J. Cell Biol.* **109:** 2097–2104.
19. Mukherjee, S., T. T. Soe, and F. R. Maxfield. 1999. Endocytic sorting of lipid analogues differing solely in the chemistry of their hydrophobic tails. *J. Cell Biol.* **144:** 1271–1284.
20. Hojjati, M. R., and X. C. Jiang. 2006. Rapid, specific, and sensitive measurements of plasma sphingomyelin and phosphatidylcholine. *J. Lipid Res.* **47:** 673–676.
21. Preiss, J., C. R. Loomis, W. R. Bishop, R. Stein, J. E. Niedel, and R. M. Bell. 1986. Quantitative measurement of sn-1,2-diacylglycerols present in platelets, hepatocytes, and ras- and sis-transformed normal rat kidney cells. *J. Biol. Chem.* **261:** 8597–8600.
22. Puri, V., J. R. Jefferson, R. D. Singh, C. L. Wheatley, D. L. Marks, and R. E. Pagano. 2003. Sphingolipid storage induces accumulation of intracellular cholesterol by stimulating SREBP-1 cleavage. *J. Biol. Chem.* **278:** 20961–20970.
23. Huan, C., M. L. Kelly, R. Steele, I. Shapira, S. R. Gottesman, and C. A. Roman. 2006. Transcription factors TFE3 and TFEB are critical for CD40 ligand expression and thymus-dependent humoral immunity. *Nat. Immun.* **7:** 1082–1091.
24. Ishitsuka, R., A. Yamaji-Hasegawa, A. Makino, Y. Hirabayashi, and T. Kobayashi. 2004. A lipid-specific toxin reveals heterogeneity of sphingomyelin-containing membranes. *Biophys. J.* **86:** 296–307.
25. Mayor, S., and F. R. Maxfield. 1995. Insolubility and redistribution of GPI-anchored proteins at the cell surface after detergent treatment. *Mol. Biol. Cell.* **6:** 929–944.

26. Thorburn, A. 2004. Death receptor-induced cell killing. *Cell. Signal.* **16:** 139–144.
27. Linn, S. C., H. S. Kim, E. M. Keane, L. M. Andras, E. Wang, and A. H. Merrill. 2001. Regulation of de novo sphingolipid biosynthesis and the toxic consequences of its disruption. *Biochem. Soc. Trans.* **29:** 831–855.
28. Schutze, S., K. Potthoff, T. Machleidt, D. Berkovic, K. Wiegmann, and M. Kronke. 1992. TNF activates NF-kappa B by phosphatidylcholine-specific phospholipase C-induced "acidic" sphingomyelin breakdown. *Cell.* **71:** 765–776.
29. Hanada, K. 2003. Serine palmitoyltransferase, a key enzyme of sphingolipid metabolism. *Biochim. Biophys. Acta.* **1632:** 16–30.
30. Meng, A., C. Luberto, P. Meier, A. Bai, X. Yang, Y. A. Hannun, and D. Zhou. 2004. Sphingomyelin synthase as a potential target for D609-induced apoptosis in U937 human monocytic leukemia cells. *Exp. Cell Res.* **292:** 385–392.
31. Separovic, D., K. Hanada, M. Y. Maitah, B. Nagy, I. Hang, M. A. Tainsky, J. M. Kraniak, and J. Bielawski. 2007. Sphingomyelin synthase 1 suppresses ceramide production and apoptosis post-photodamage. *Biochem. Biophys. Res. Commun.* **358:** 196–202.
32. Ko, Y-G., J-S. Lee, Y-S. Kang, J-H. Ahn, and J-S. Seo. 1999. TNF-α-mediated apoptosis is initiated in caveolae-like domains. *J. Immunol.* **162:** 7217–7223.
33. Triantafilou, M., K. Miyake, D. T. Golenbock, and K. Triantafilou. 2002. Mediators of innate immune recognition of bacteria concentrate in lipid rafts and facilitate lipopolysaccharide-induced cell activation. *J. Cell Sci.* **115:** 2603–2611.
34. Basu, A. 2003. Involvement of protein kinase C-delta in DNA damage-induced apoptosis. *J. Cell. Mol. Med.* **7:** 341–350.
35. Murriel, C. L., and D. Mochly-Rosen. 2003. Opposing roles of delta and epsilonPKC in cardiac ischemia and reperfusion: targeting the apoptotic machinery. *Arch. Biochem. Biophys.* **420:** 246–254.
36. Hannun, Y. A., and C. Luberto. 2000. Ceramide in the eukaryotic stress response. *Trends Cell Biol.* **10:** 73–80.
37. Kolesnick, R. 2002. The therapeutic potential of modulating the ceramide/sphingomyelin pathway. *J. Clin. Invest.* **110:** 3–8.
38. Wyllie, A. H., J. F. Kerr, and A. R. Currie. 1980. Cell death: the significance of apoptosis. *Int. Rev. Cytol.* **68:** 251–306.
39. Geng, Y. J., and P. Libby. 2002. Progression of atheroma: a struggle between death and procreation. *Arterioscler. Thromb. Vasc. Biol.* **22:** 1370–1380.
40. Tabas, I. 2005. Consequences and therapeutic implications of macrophage apoptosis in atherosclerosis: the importance of lesion stage and phagocytic efficiency. *Arterioscler. Thromb. Vasc. Biol.* **25:** 2255–2264.
41. Arai, S., J. M. Shelton, M. Chen, M. N. Bradley, A. Castrillo, A. L. Bookout, P. A. Mak, P. A. Edwards, D. J. Mangelsdorf, P. Tontonoz, et al. 2005. A role for the apoptosis inhibitory factor AIM/Spalpha/Api6 in atherosclerosis development. *Cell Metab.* **1:** 201–213.
42. Liu, J., D. P. Thewke, Y. R. Su, M. F. Linton, S. Fazio, and M. S. Sinensky. 2005. Reduced macrophage apoptosis is associated with accelerated atherosclerosis in low-density lipoprotein receptor-null mice. *Arterioscler. Thromb. Vasc. Biol.* **25:** 174–179.
43. Johnson, J. L., A. H. Baker, K. Oka, L. Chan, A. C. Newby, C. L. Jackson, and S. J. George. 2006. Suppression of atherosclerotic plaque progression and instability by tissue inhibitor of metalloproteinase-2: involvement of macrophage migration and apoptosis. *Circulation.* **113:** 2435–2444.
44. Han, S., C. P. Liang, T. DeVries-Seimon, M. Ranalletta, C. L. Welch, K. Collins-Fletcher, D. Accili, I. Tabas, and A. R. Tall. 2006. Macrophage insulin receptor deficiency increases ER stress-induced apoptosis and necrotic core formation in advanced atherosclerotic lesions. *Cell Metab.* **3:** 257–266.
45. Ikonen, E., and S. Vaini. 2005. Lipid microdomains and insulin resistance: is there a connection? *Sci. STKE.* **268:** 1–3.